A rebuilding time model for Pacific salmon

Michael R. O'Farrell

William H. Satterthwaite

Fisheries Ecology Division
Southwest Fisheries Science Center
National Marine Fisheries Service
National Oceanic and Atmospheric Administration
110 McAllister Way
Santa Cruz, CA 95060, USA

Corresponding author: M.R. O'Farrell
email: michael.ofarrell@noaa.gov; tel: 831.420.3976; fax: 831.420.3977

Abstract

We describe a new model developed for the purpose of projecting rebuilding periods for overfished Pacific salmon stocks as defined by the Pacific Fishery Management Council. The model has relatively low data requirements as it relies on past estimates of abundance to project future abundance, accounting for positive lag-1 autocorrelation if there is evidence of its existence. Replicate applications of the model allow for computation of the probability of achieving rebuilt status in future years. Application to simulated abundance and escapement data suggested that model-projected rebuilding times generally corresponded to simulated rebuilding times as raw errors were median unbiased. Simulations also suggested that results were generally robust to parameter misspecification and that increased levels of lag-1 autocorrelation in abundance were associated with longer rebuilding periods. The application of the model to five overfished stocks in 2018-2019 illustrated the differences in projected rebuilding times under alternative rebuilding management strategies. The model filled a need for relatively rapid assessment of alternative rebuilding strategies for Pacific salmon stocks, a need that will likely remain given current biological reference points and fluctuations in salmon abundance.

Keywords: Overfished, Rebuilding period, Salmon,

1. Introduction

Ending overfishing and rebuilding overfished stocks is a priority for many countries, however reducing fishing mortality rates and rebuilding stock biomass has socioeconomic consequences (NRC, 2014). The choice of management strategies for rebuilding depleted stocks involves considering tradeoffs between the severity of fishery reductions (e.g., in terms of catch or effort) and the duration of such reductions (Hilborn et al., 2011; Wetzel and Punt, 2016). The United States Magnuson-Stevens Fishery Conservation and Management Act[1] (hereafter MSA) requires that rebuilding plans for overfished stocks specify rebuilding periods. As of June 2020, there were 49 overfished stocks in the United States, all of which require the development of a rebuilding plan and an estimated rebuilding period.

Since 2012, the Pacific Coast Salmon Fishery Management Plan (FMP; PFMC, 2016) has specified that a stock meets the criteria for overfished status if the geometric mean of the most recent three years of spawner escapement falls below the minimum stock size threshold (MSST). The MSST ranges by stock from 0.50 to 0.75 of the spawner escapement that is expected, on average, to produce maximum sustainable yield (S_{MSY}). The default criterion for achieving rebuilt status is a geometric mean of the most recent three years of spawner escapement meeting or exceeding S_{MSY}. The use of a multi-year criteria for determining overfished and rebuilt status recognizes the dynamics of short-lived and semelparous salmon populations that can exhibit large annual fluctuations.

In 2018, five Pacific salmon stocks, two Chinook and three coho, met the criteria for overfished status and rebuilding plans were required to be prepared for Pacific Fishery Management Council (PFMC) consideration within one year. In the salmon FMP, there are currently 25 stocks with specified MSST and S_{MSY} values that are used to assess overfished and rebuilt status. There are a substantial number of other stocks in the FMP that do not have these associated reference points because they are either listed under the United States Endangered Species Act, are managed as part of a stock complex, or are a hatchery stock. While the number of overfished salmon stocks in 2018 was unprecedented for the PFMC, if the current stock reference points (e.g., MSST, S_{MSY}) and overfished criterion were applied to past years, this number of overfished stocks would be somewhat unremarkable (Figure 1). Hence, the ability to produce rebuilding plans with projections of rebuilding periods for multiple stocks within a short time frame will likely be necessary into the future. Prior to 2018 there were no accepted methods for projecting the rebuilding period for salmon stocks. This contrasts with some FMPs where very specific guidelines are in place for developing rebuilding analyses. For example, terms of reference have been developed for conducting rebuilding analyses for Pacific Coast groundfish, using standardized software (developed by A. Punt, University of Washington, USA, based on Punt and Ralston, 2007), which includes calculation of minimum and maximum times to recovery (PFMC, 2018).

In this paper, we describe a Monte Carlo simulation approach developed to predict rebuilding periods for overfished salmon stocks. The approach has low data requirements and therefore can be applied to a wide variety of stocks with different levels of data richness. It relies upon past estimates of abundance to project future abundance, accounting for positive lag-1 autocorrelation

[1] https://www.fisheries.noaa.gov/resource/document/magnuson-stevens-fishery-conservation-and-management-act

if the time series of abundance suggests it exists. This autocorrelation may implicitly capture the effects of an autocorrelated environment or other biological processes operating on a short time scale, without explicitly modeling them. It does not require information on stock productivity or production capacity. The model structure is consistent with the annual salmon season planning process where stock-specific forecasts of abundance are applied to control rules that specify maximum allowable exploitation rates from all salmon-directed fisheries (e.g., commercial, recreational, and tribal). Harvest models are then used to project stock-specific exploitation rates and spawner escapements, given the planned salmon fisheries. The rebuilding time model explicitly accounts for abundance forecasting error, exploitation rate implementation error, and spawner escapement observation error. Implementation of this method in 2018-2019 established projected rebuilding times for alternative rebuilding strategies, as required by the MSA (PFMC, 2019a-e). In addition, the projected rebuilding times were used by stakeholders and fishery managers to evaluate alternative rebuilding strategies by weighing potential reductions in the salmon fishery against the time it would take to rebuild the stocks.

After specifying the rebuilding time model, model performance is evaluated under alternative parameter assumptions, data ranges, and levels of autocorrelation in abundance through application to simulated data. The model implementation for the five overfished stocks in years 2018-2019 is then described. We end with a discussion of potential modifications to model structure that could be considered in future applications.

2. Material and methods

2.1 Model Specification

Log-scale, pre-fishery ocean abundance in year *t*, $\log(N_t)$, is characterized by lag-1 autocorrelated draws from a Normal distribution with parameters estimated from past stock abundances. Abundance is specified in terms of adult (age ≥ 3) spawner equivalent units (PFMC 2016). Simulated log-scale abundance in year *t* is a function of log abundance in the previous year $\log(N_{t-1})$, the lag-1 autocorrelation coefficient $\hat{\rho}$, and a draw from the distribution characterizing past abundance on the log scale Y_t,

$$\log(N_t) = \hat{\rho}[\log(N_{t-1})] + (1-\hat{\rho})Y_t, \qquad (1)$$

with

$$Y_t \sim \text{Normal}\left[\log(\bar{X}) - 0.5\hat{\sigma}^2_{\log(X)}, \sqrt{\frac{(1-\rho^2)\hat{\sigma}^2_{\log(X)}}{(1-\rho)^2}}\,\right]. \qquad (2)$$

Here $\bar{X}$ is the arithmetic mean of the estimated abundance time series and $\hat{\sigma}^2_{\log(X)}$ is the variance of the log-transformed estimated abundance time series. Point Estimates of $\log(\bar{X})$, $\hat{\sigma}_{\log(X)}$, and $\hat{\rho}$ are obtained from the available abundance time series for the overfished stock. If $\hat{\rho}$ is estimated to be negative, $\hat{\rho}$ is assumed to be zero. The standard deviation term in equation 2 is derived from the expression for the standard deviation of a sum of two random variables. Simulated log-scale abundance in year *t* is then back-transformed to the arithmetic scale, $N_t = \exp[\log(N_t)]$.

Allowable fishing mortality rates are specified for many Pacific salmon stocks on the basis of preseason ocean abundance forecasts, $\widehat{N}$. To account for abundance forecast errors, the forecast ocean abundance is represented by a draw from a lognormal distribution

$$\widehat{N}_t \sim \text{Lognormal}[\log(N_t) - 0.5\sigma^2_{\log(\widehat{N})},\ \sigma_{\log(\widehat{N})}] \qquad (3)$$

where the bias corrected mean and standard deviation are specified on the log scale. The log-scale standard deviation was determined by the coefficient of variation (CV) for abundance forecast error $\text{CV}_{\widehat{N}}$,

$$\sigma_{\log(\widehat{N})} = \sqrt{\log\left(1 + \text{CV}^2_{\widehat{N}}\right)}, \qquad (4)$$

where the $\text{CV}_{\widehat{N}}$ is a model parameter that can either be specified or estimated from past forecast errors.

A control rule is applied to the ocean abundance forecast $\widehat{N}_t$ to determine the allowable exploitation rate, $\widehat{F}_t$. Note that, as is common practice in salmon management models, *F* is expressed as an annual fraction rather than an instantaneous rate. The model allows for flexibility in the form of control rules, which are user-specified. The exploitation rate accounts for all fishing-related mortality in the ocean, estuary, and freshwater habitats. The ˆ notation for $\widehat{F}$ indicates that this exploitation rate is a target exploitation rate derived from an abundance forecast.

Simulated adult spawner escapement E_t is computed from the pre-fishery ocean abundance and the realized exploitation rate F_t

$$E_t = N_t \times (1 - F_t). \qquad (5)$$

The realized exploitation rate is a function of the allowable exploitation rate and expected errors in implementation. Thus, F_t is determined by a random draw from a beta distribution

$$F_t \sim \text{Beta}(\alpha, \beta) \qquad (6)$$

with parameters

$$\alpha = \frac{1 - \widehat{F}_t(1 + \text{CV}^2_F)}{\text{CV}^2_F} \qquad (7)$$

and

$$\beta = \frac{\frac{1}{\widehat{F}_t} - 2 + \widehat{F}_t + (\widehat{F}_t - 1)\text{CV}^2_F}{\text{CV}^2_F} \qquad (8)$$

(Winship et al., 2013). The coefficient of variation for the exploitation rate implementation error, CV_F, is a model parameter that can either be specified or estimated from past exploitation rate implementation errors.

Adult spawner escapement for most salmon stocks is not directly enumerated but rather is estimated with associated observation error. To account for this error, escapement estimates $\hat{E}_t$ are drawn from a lognormal distribution

$$\hat{E} \sim \text{Lognormal}[\log(E_t) - 0.5\sigma^2_{\log(\hat{E})},\ \sigma_{\log(\hat{E})}] \qquad (9)$$

where the bias corrected mean and standard deviation are specified on the log scale. The log-scale standard deviation was computed in the same manner as equation 4, with the parameter $\text{CV}_{\hat{E}}$ characterizing the escapement observation error CV.

A single implementation of this model results in projected spawner escapement estimates for a pre-specified number of years into the future. Rebuilt status for an individual replicate simulation occurs when the geometric mean of $\hat{E}$ computed over the previous three years first exceeds S_{MSY} (PFMC, 2016). To assess the probability of reaching rebuilt status by year, a large number of replicate simulations (e.g., 10,000 when applied to the five overfished stocks in 2018-2019) are performed and the proportion of replicates that meet the rebuilt criterion in each future year are computed. The probability of achieving rebuilt status in year *t* is the cumulative probability of achieving a 3-year geometric mean greater than or equal to S_{MSY} by year *t*. The model has been implemented in the R programming environment (R Core Team, 2019) and is available from the corresponding author upon request.

2.2 Application to Simulated Data

Rebuilding time model performance was evaluated by applying the model to simulated abundance and escapement data. Parameter values assumed in data simulations follow those estimated for Klamath River fall Chinook salmon, the indicator stock for the Southern Oregon Northern California Chinook Stock Complex (PFMC, 2016) and one of the five stocks declared overfished in 2018 (Table 1).

2.2.1 Data generation process

Starting log-scale abundance (year 1) for all replicate simulations was set to the mean of log-scale Klamath River fall Chinook abundance [$\log(\bar{X})$ in Table 1]. Ocean abundance and observed escapement were projected for 200 years, following equations 1-9, the parameter set in Table 1, and the Klamath River fall Chinook exploitation rate control rule (Figure 2).

Running 3-year geometric means of simulated time series of escapement observations were computed for the 200 year dataset to determine years for which the criteria for overfished status was met. Overfished status resulted for year *t* if the geometric mean of escapement observations in *t*-2, *t* -1, and *t* was less than or equal to the MSST. The entire simulated data series was discarded if (1) the criteria for overfished status was not met over the 200 year simulation or (2) the stock was rebuilt in the year following overfished criteria being met as the stock would be rebuilt prior to development of a rebuilding plan.

Simulated abundance "data" prior to and immediately following the overfished determination were retained. The rest of the 200 year simulated abundance series was then discarded. The data retained following the overfished determination reflect management lags between the overfished determination and the implementation of the rebuilding plan, which is described in greater detail below.

The rebuilding time was determined from the simulated escapement time series by determining the first year following the overfished determination for which the three year geometric mean of escapement was greater than or equal to S_{MSY}. Applying realistic lags in the management process necessitates that year 1 of the rebuilding period would correspond to 2 years following the first escapement year in which overfished status was reached. For example, if the simulated escapement time series met the criteria for overfished in escapement year 25, the rebuilding plan would include escapement data through escapement year 27. A rebuilding time of one year would then correspond to meeting the criteria for rebuilt status in escapement year 27.

To explore the effects of data set length on rebuilding model performance, simulated abundance time series of lengths 15 and 30 years were generated. Simulated abundance data for the 15 year data length spanned year t -13 to t +1, where $t = 0$ is the first year the stock met the overfished criterion. Simulated abundance data for the 30 year data length spanned abundances in year t -28 to t +1. Data series of these lengths are currently representative of many salmon stocks along the U.S. West Coast.

To explore the effects of the level of lag-1 autocorrelation on rebuilding model performance, abundance was simulated for three levels of ρ: 0.0, 0.3, and 0.7 (Table 1). 5,000 simulated datasets were retained for each of the six scenarios, describing pairwise combinations of data series length (15, 30 years) and ρ (0.0, 0.3, and 0.7), for a total of 30,000 data sets.

2.2.2 Application of the rebuilding time model to simulated data

Values of $\log(\bar{X})$, $\hat{\sigma}_{\log(X)}$, and $\hat{\rho}$ were estimated from the simulated data. The management strategy used for application of the rebuilding time model to these simulated data sets is the control rule depicted in Figure 2. 6,000 replicate applications of the rebuilding time model were associated with each of the 30,000 simulated data series. The parameters $\log(\bar{X})$, $\hat{\sigma}_{\log(X)}$, and $\hat{\rho}$, and the most recent abundance value on the log scale, $\log(N)$, were derived from the simulated data series. The probability of achieving rebuilt status by year was computed across 6,000 replicate applications of the rebuilding time model for each of the 5,000 simulated data series associated with a given data series length and value of ρ. The projected rebuilding time was defined as the first year in which the probability of being rebuilt was ≥ 0.5.

5,000 pairs of simulated rebuilding times (s) and rebuilding time model-projected rebuilding times (p) were used estimate distributions of raw error ($p - s$) and to assess model performance. Positive values of raw error indicate that model-projected rebuilding times were longer than simulated rebuilding times, while negative raw errors indicate the converse.

Parameter	Value	Definition
S_{MSY}	40700	Maximum sustainable yield spawner escapement
MSST	30525	Minimum Stock Size Threshold
$\mathrm{CV}_{\hat{N}}$	0.2	Abundance forecast error CV
CV_{F}	0.1	Exploitation rate implementation error CV
$\mathrm{CV}_{\hat{E}}$	0.2	Escapement observation error CV
$\log(\bar{X})$	11.518	Log-scale mean ocean abundance
$\hat{\sigma}_{\log(X)}$	0.764	Standard deviation of log-scale abundance
$\hat{\rho}$	0.0, 0.3, 0.7	Lag-1 autocorrelation coefficient

Table 1. Parameter values used to simulate abundance and escapement data and determine overfished and rebuilt status from simulated escapement data. The CV values in the table were used both in the simulation of data and the application of the rebuilding times model to the simulated data.

To evaluate model performance when parameters $\mathrm{CV}_{\hat{N}}$, CV_{F}, and $\mathrm{CV}_{\hat{E}}$ are mis-specified, abundance and escapement data were simulated with values of these parameters that differed from the values assumed for the rebuilding time model. Data were simulated with parameter values $\mathrm{CV}_{\hat{N}} = 0.6$, $\mathrm{CV}_{F} = 0.2$, and $\mathrm{CV}_{\hat{E}} = 0.5$, which are higher levels of abundance forecast error, exploitation rate implementation error, and escapement observation error, respectively, than values assumed for the rebuilding time model ($\mathrm{CV}_{\hat{N}} = 0.2$, $\mathrm{CV}_{F} = 0.1$, and $\mathrm{CV}_{\hat{E}} = 0.2$). Model performance was again assessed by examination of distributions of raw error over 5000 pairs of simulated rebuilding times and model-projected rebuilding times.

Simulated data were also used to assess the effect of lag-1 autocorrelation on simulated and model-projected rebuilding times. We examined the distributions of rebuilding times resulting from simulations assuming $\rho = 0$, $\rho = 0.3$, and $\rho = 0.7$. The effect of estimated ρ on projections made with the rebuilding time model applied to simulated data was also examined; model-projected rebuilding times were plotted as a function of $\hat{\rho}$ (the lag-1 autocorrelation coefficient estimated from simulated abundance data). There were a total of 15,000 pairs of projected rebuilding times and $\hat{\rho}$ (5000 pairs for each level of specified ρ). Running medians of projected rebuilding times were computed over the range of $\hat{\rho}$.

2.3 Application to overfished stocks in 2018-2019

The rebuilding time model was applied to the five Pacific salmon stocks declared overfished in 2018. Values of $\bar{X}$, $\hat{\sigma}_{\log(X)}$, and $\hat{\rho}$ were estimated using available abundance data prior to the overfished declaration. Data series spanned 14 years for Queets River natural coho, Snohomish River natural coho, and Strait of Juan de Fuca natural coho, 36 years for Sacramento River fall Chinook, and 34 years for Klamath River fall Chinook. Assumed values of $\mathrm{CV}_{\hat{N}}$, CV_{F}, and $\mathrm{CV}_{\hat{E}}$ are equivalent to those found in Table 1 and did not vary between stocks.

Rebuilding times were assessed under three rebuilding alternatives for each of the overfished stocks. Alternative I was the status quo fishery management approach that is used in most years for the planning of fisheries.

Alternative II was a fishery management strategy that featured reduced exploitation rates or increased escapement targets relative to Alternative I. The Alternative II management strategies differed between the five overfished stocks. For Klamath River fall Chinook and Sacramento River fall Chinook, Alternative II specified reduced exploitation rates at all levels of forecast abundance (PFMC, 2019a,c). Figure 3 displays Alternative II in relation to Alternative I for Sacramento River fall Chinook. The relationship between Alternative I and Alternative II was similar in form for Klamath River fall Chinook, but with smaller reductions in allowable exploitation rates between Alternatives I and II (PFMC, 2019a). For Queets River natural coho, Alternative II specified lower allowable exploitation rates at low levels of abundance ($< 7{,}250$) relative to Alternative I (PFMC, 2019b). For Strait of Juan de Fuca natural coho, Alternative II specified a maximum exploitation rate of 0.10 for the Southern United States fishery, whereas there was no such exploitation rate cap under Alternative I (PFMC, 2019e). For Snohomish River natural coho, Alternative II specified an escapement goal of 55,000 relative to the goal of 50,000 for Alternative I (PFMC, 2019d).

The third rebuilding alternative was a zero exploitation rate strategy that was used to establish T_{MIN}, the minimum projected rebuilding time. See PFMC (2019a-e) for detailed descriptions of the stock-specific rebuilding alternatives.

For each overfished stock the probability of achieving rebuilt status was projected for the three alternatives. The probability of achieving rebuilt status for each year within a 10 year window were based on 10,000 replicate simulations. The projected rebuilding time for an alternative was specified as the first year for which the probability of rebuilt status was ≥ 0.50.

3 Results

3.1 Application to simulated data

Estimated parameters for the rebuilding time model varied around the values used to simulate abundance data (Figure 4). Estimated parameters varied more around assumed parameter values when the data series was shorter. Estimated $\hat{\rho}$ were generally lower than values assumed for data simulation under both data length scenarios, though the differences were more pronounced for the shorter, 15 year data series simulations. For cases where data were simulated with $\rho = 0$, the median value of $\hat{\rho}$ was also zero, though per model convention, $\hat{\rho}$ is assigned to zero if the estimated lag-1 autocorrelation coefficient is negative. Estimates of the log-scale mean of abundance were generally unbiased across scenarios, though estimates were more variable when the specified ρ in simulations was larger. Estimates of the standard deviation of log-scale abundance were lower than parameter values specified in simulations under higher levels of autocorrelation. This effect was more pronounced for the shorter data length scenario.

Biased parameter estimates did not lead to bias in the median of raw error distributions computed for simulated and model-projected rebuilding times as median raw errors were zero in all cases (Figure 5). The variation in raw error was larger for the scenarios with $\rho = 0.7$ relative to lower levels of ρ. Distributions of raw error were negatively skewed (median exceeded the mean) indicating that negative errors (model-projected rebuilding times shorter than simulated rebuilding times) tended to be larger than positive errors (model-projected rebuilding times longer than simulated rebuilding times).

There appear to be generally small effects on rebuilding time raw errors when parameters $\mathrm{CV}_{\hat{N}}$, CV_{F}, and $\mathrm{CV}_{\hat{E}}$ assumed for rebuilding time projections were misspecified (Figure 6). Distributions of raw error between model-projected and simulated rebuilding times had median values of zero. Distributions of raw errors tended to be negatively skewed, indicating that negative errors (model-projected rebuilding times shorter than simulated rebuilding times) tended to be larger than positive errors (model-projected rebuilding times longer than simulated rebuilding times).

Both simulated and model-projected rebuilding times increased with higher levels of lag-1 autocorrelation in abundance. Assuming $\rho = 0$, the median simulated rebuilding time was three years (Figure 7a). Median rebuilding time increased to four years with $\rho = 0.3$ and five years with $\rho = 0.7$. This pattern was also observed when applying the rebuilding time model to simulated data. Median model-projected rebuilding times ranged from a low of three years when $\hat{\rho} < 0.2$ to a high of six years when $\hat{\rho} \geq 0.8$ (Figure 7b).

3.2 Application to overfished stocks in 2018-2019

Figure 8 displays the probability of achieving rebuilt status for five overfished salmon stocks in 2018-2019. Rebuilding times varied from a minimum of one year (under the T_{MIN} scenario for Klamath River fall Chinook and Queets River natural coho) to a maximum of six years (under Alternative I for Strait of Juan de Fuca natural coho).

The status quo management strategy (Alternative I) resulted in the longest rebuilding times and the T_{MIN} scenario the shortest rebuilding times. For the coho stocks, there were small differences in rebuilding probabilities between Alternatives I and II, reflecting the similarity of the control rules underlying those Alternatives (PFMC, 2019b,d,e). The differences between rebuilding probabilities for the T_{MIN} scenario and Alternative I were small for the coho stocks relative to the Chinook stocks, which reflects the lower overall exploitation rates generally experienced for these coho stocks. Accuracy of the rebuilding time projections cannot be assessed at this time as none of the five stocks have met the criteria for rebuilt status at the time of publication.

4. Discussion

Projected rebuilding periods are used to aid the rebuilding strategy decision making process for stakeholders and fishery managers. The rebuilding time model described here has modest data requirements, which is desirable because sufficient data do not readily exist for many salmon stocks to fit stock-recruitment relationships and develop more complex population dynamics models. While in some cases having a more explicit link between the spawning stock and recruits to the fishery would be desirable, for stocks with substantial hatchery supplementation, spawning stock size may have little influence on recruitment. More complex models that directly account for natural and hatchery production (e.g., Winship et al., 2013) could be developed to assess rebuilding periods. For stocks with little hatchery supplementation, a simulation approach analogous to that described in Freshwater et al. (2019) could also be used to assess alternative rebuilding plans. Implementing models such as these requires both substantially more data and development time than the rebuilding time model described here, which may be infeasible given short statutory timelines. The use of autocorrelated abundances provides an empirically-driven method that may implicitly capture some environmental or biological effects that are not explicitly modeled, without involving the covariate selection challenges that often accompany use of environmental covariates (Winship et al., 2015). Prior work on assessment of rebuilding periods has shown that results can be highly sensitive to the methods used to simulate recruitment (Punt and Methot, 2005; Holt and Punt, 2009).

Although this model was developed for the specific needs of the PFMC and its management of Pacific salmon, our approach may be applicable in other regions, or to other short-lived species. In Canada, following passage of the revised Fisheries Act[2] in 2019, it will be necessary to assess the majority of fish stocks against Limit Reference Points (LRPs) and develop rebuilding plans for stocks that fall below these limits. There were previous, not legally-binding, calls for rebuilding of depleted stocks in the Wild Salmon Policy[3] of 2005, but appropriate analyses were only possible for a few relatively data-rich stocks (e.g., Pestal et al. 2011; Grant et al. 2020), with the lack of suitable data for estimating stock-recruitment relationships hindering both the determination of LRPs and the analysis of harvest control rules for most other stocks. Alternative approaches like setting LRPs based on percentiles of past escapement (e.g., Clark et al., 2014; Holt et al., 2018) along with our approach to closed loop simulations exploring rebuilding under different harvest control rules may be a suitable approach in such cases.

Elements of our approach may also be useful for other short-lived species. Within the PFMC realm, a rebuilding plan was recently required for the northern subpopulation of Pacific sardine (*Sardinops sagax caerulea*). With limited time to produce the rebuilding plan, and at least in part because of a perceived need to estimate a stochastic reference point reflecting the biomass corresponding to sustainable yield (B_{MSY}) to serve as the rebuilding target, the analysts used a minimally modified version of the rebuilding software developed for long-lived groundfish (Hill et al., 2020). This approach was endorsed by the PFMC's Scientific and Statistical Committee (PFMC, 2020), but they noted "challenges associated with projecting rebuilding for a highly dynamic species whose recruitment seems to be largely driven by environmental factors" and high sensitivity to assumptions about future environmental/productivity regimes. Ultimately, the PFMC adopted a rebuilding target based on the "cutoff" parameter in the harvest control rule defined in the Coastal Pelagic Species Fishery Management Plan (PFMC, 2019f) rather than an estimate of stochastic B_{MSY}. With a pre-specified rebuilding target in place, an approach similar to ours might have been suitable, and its low computational demands coupled with relatively few parameters requiring sensitivity analyses might have allowed exploration of a broader range of future productivity scenarios.

Our simulations suggest that longer rebuilding times are associated with higher levels of autocorrelation, but we have not tested whether this conclusion holds over different assumptions about the operating model (e.g., incorporating density dependent recruitment). This is not unexpected because escapement, and likely pre-fishery abundance, must be low to meet the

---

[2] https://www.parl.ca/LegisInfo/BillDetails.aspx?Language=E&billId=9630814
[3] https://www.pac.dfo-mpo.gc.ca/fm-gp/salmon-saumon/wsp-pss/index-eng.html

criteria for overfished status. Populations with high levels of autocorrelation would not be expected to exhibit rapid increases in abundance or a bonanza recruitment that could lead to rapid rebuilding. Estimates of the autocorrelation coefficient from simulated data were biased low when simulations assumed $\rho > 0$. The bias was more pronounced for the shorter data series and the higher levels of autocorrelation in the simulated data, a result consistent with expectations (e.g., Bence, 1995). While this did not strongly affect rebuilding model performance, as raw error distributions were median unbiased (Figure 5), the distributions were negatively skewed under some scenarios, most notably for $\rho = 0.7$. This result implies a negative bias in mean raw error (shorter model-projected rebuilding times relative to simulated rebuilding times) which is consistent with our observation that shorter rebuilding times are associated with lower levels of lag-1 autocorrelation in abundance.

Rebuilding time model projections were generally robust to parameter misspecification. Assuming lower levels of abundance forecast error $\mathrm{CV}_{\hat{N}}$, exploitation rate implementation error CV_{F}, and escapement estimation error $\mathrm{CV}_{\hat{E}}$ did not result in large differences between model projected and simulated rebuilding times. Obtaining direct estimates of these parameters can be difficult for some populations owing to data deficiencies and may need to be assumed when applying the rebuilding time model to many stocks.

When applying this model to Sacramento River fall Chinook and Klamath River fall Chinook salmon, two additional model variants were considered. The first variant was to account for bias in abundance forecasts. This variant was pursued because the forecasted index of abundance for Sacramento River fall Chinook has frequently exceeded the postseason estimate. To account for this bias, the log of the ratio between the preseason forecast and postseason estimate of abundance was added to the mean term in equation 3, i.e., $\log(N_t) - 0.5\sigma^2_{\log(\hat{N})} + r$, where r is drawn, with replacement, from the set of log ratios. Rebuilding time projections that incorporated abundance forecast bias for Sacramento River fall Chinook were somewhat longer than projections that did not take this bias into account (PFMC, 2019c). In contrast, rebuilding time projections from the base model and the abundance forecast bias variant were nearly identical for Klamath River fall Chinook, reflecting the relative lack of bias in abundance forecasts observed for this stock (PFMC, 2019a). The second variant of the rebuilding model considered was to characterize past abundance based on more recent abundance estimates to account for changes in stock productivity over the course of the data range. For this variant, $\log(\bar{X})$ and $\hat{\sigma}_{\log(X)}$ were estimated from contemporary abundance data while $\hat{\rho}$ was estimated using the full abundance data set. Application of this model variant to Sacramento River fall Chinook salmon resulted in longer rebuilding times relative to the base model implementation (PFMC, 2019c), whereas rebuilding times were similar across both model implementations for Klamath River fall Chinook salmon (PFMC, 2019a). We note that rebuilding time results could be highly sensitive to the choice of a "cut off" for years to consider as part the contemporary period.

One feature of the rebuilding time model that does not reflect the management of Pacific salmon fisheries is the lack of explicit accounting for weak stock management. Exploitation rate projections for some stocks are frequently lower than the allowable exploitation rate specified by their control rule because of fishery constraints from comingled stocks. The rebuilding model assumes that the maximum exploitation rate specified by the control rule is targeted each year. While the effect of weak stock management on rebuilding model performance was not explored here, we would expect that stocks that are frequently prevented from achieving maximum allowable exploitation rates owing to comingled weaker stocks would have shorter rebuilding times than model projections.

In conclusion, we specified and evaluated a new model used to project rebuilding periods for Pacific salmon. Application to simulated data, suggested median unbiased projections of the rebuilding period under scenarios with and without misspecification of assumed parameters. The model was successfully applied in practice and was used to establish projected rebuilding times for five salmon stocks, though the accuracy of those projections is as yet unknown. While the model was designed for Pacific salmon, accounting for the fishery management context and typical data associated with salmon stocks, aspects of this approach may find use for other species. In particular, using past estimates of abundance while accounting for autocorrelation could find utility for other short-lived fish stocks. Such an approach represents one way to incorporate environmental or ecosystem effects into projections of rebuilding periods with very modest data requirements.

5. Acknowledgments

We would like to thank members of the PFMC's Salmon Technical Team and Scientific and Statistical Committee for providing input and review of the rebuilding time model as it was being developed. E.J. Dick and John Field provided many helpful suggestions during manuscript development, and two anonymous reviewers made several helpful suggestions that improved the paper. Will Atlas, Cameron Freshwater, Carrie Holt, and Jordan Watson provided valuable insights into salmon management beyond the PFMC. Special thanks go to Ole Shelton for ideas on implementing the autocorrelated draws from a distribution of abundance. This research did not receive any specific grant from funding agencies in the public, commercial, or not-for-profit sectors.

6. References

Bence, J.R., 1995. Analysis of short time series: correcting for autocorrelation. Ecology 76, 628-639. https://doi.org/10.2307/1941218

Clark, R.A., D.M. Eggers, A.R. Munro, S.J. Fleischman, B.G. Bue, and J.J. Hasbrouck. 2014. An evaluation of the percentile approach for establishing sustainable escapement goals in lieu of stock productivity information. Alaska Department of Fish and Game, Fishery Manuscript Series No. 14-06, Anchorage. Available from: http://www.adfg.alaska.gov/FedAidPDFs/FMS14-06.pdf

Freshwater, C., S.C. Anderson, K.R. Holt, A.-M. Huang, and C.A. Holt. 2019. Weakened portfolio effects constrain management effectiveness for population aggregates. Ecological Applications 29, e01966. 10.1002/eap.1966

Grant, S.C.H., Holt, C.A., Pestal, G., Davis, B.M. and MacDonald, B.L. 2020. The 2017 Fraser Sockeye Salmon (Oncorhynchus nerka) Integrated Biological Status Re-Assessments Under the Wild Salmon Policy Using Standardized Metrics and Expert Judgment. DFO Can. Sci. Advis. Sec. Res. Doc. 2020/035. vii + 211 p. Available from: https://www.dfo-mpo.gc.ca/csas-sccs/Publications/ResDocs-DocRech/2020/2020_038-eng.pdf

Hilborn, R., I.J., Stewart, T.A., Branch, and O.P. Jensen 2011. Defining trade-offs among conservation, profitability, and food security in the California Current bottom-trawl fishery. Conservation Biology 26, 257–266. https://doi.org/10.1111/j.1523-1739.2011.01800.x

Hill, K.T., P.T. Kuriyama, and P.R. Crone. 2020. Pacific Sardine Rebuilding Analysis Based on the 2020 Stock Assessment. National Marine Fisheries Service, Southwest Fisheries Science Center, Fisheries Resources Division, La Jolla, CA 92037. Available from: https://www.pcouncil.org/documents/2020/08/g-1-a-nmfs-report-1-pacific-sardine-rebuilding-analysis-based-on-the-2020-stock-assessment.pdf/

Holt, C.A., and A.E. Punt. 2009. Incorporating climate information into rebuilding plans for overfished groundfish species of the U.S. west coast. Fisheries Research 100, 57-67. doi:10.1016/j.fishres.2009.03.002

Holt, C.A., Davis, B., Dobson, D., Godbout, L., Luedke, W., Tadey, J., and Van Will, P. 2018. Evaluating Benchmarks of Biological Status for Data-limited Conservation Units of Pacific Salmon, Focusing on Chum Salmon in Southern BC. DFO Can. Sci. Advis. Sec. Res. Doc. 2018/011. ix + 77 p. Available from: https://www.dfo-mpo.gc.ca/csas-sccs/Publications/ResDocs-DocRech/2018/2018_011-eng.html

NRC (National Research Council). 2014. Evaluating the Effectiveness of Fish Stock Rebuilding Plans in the United States. Washington, DC: The National Academies Press. https://doi.org/10.17226/18488.

Pestal, G., Huang, A-M., Cass, A. and the FRSSI Working Group. 2012. Updated Methods for Assessing Harvest Rules for Fraser River Sockeye Salmon (Oncorhynchus nerka). DFO Can. Sci. Advis. Sec. Res. Doc. 2011/133. viii + 175 p. Available from: https://waves-vagues.dfo-mpo.gc.ca/Library/347368.pdf

PFMC (Pacific Fishery Management Council). 2016. Pacific Coast Salmon Fishery Management Plan for Commercial and Recreational Salmon Fisheries off the Coasts of Washington, Oregon, and California as Amended through Amendment 19. PFMC, Portland, OR. 91 p. Available from: http://www.pcouncil.org/wp-content/uploads/2016/03/FMP-through-A-19_Final.pdf

PFMC (Pacific Fishery Management Council). 2018. Terms of Reference for the Groundfish Rebuilding Analysis for 2019-20. PFMC, Portland, OR. 19 p. Available from: https://www.pcouncil.org/wp-content/uploads/2018/06/GF_Rebuild_ToR_2019-20_Final.pdf

PFMC (Pacific Fishery Management Council). 2019a. Salmon Rebuilding Plan for Klamath River Fall Chinook. Pacific Fishery Management Council, 7700 NE Ambassador Place, Suite 101, Portland, Oregon 97220-1384. Available from: https://www.pcouncil.org/documents/2019/07/klamath-river-fall-chinook-salmon-rebuilding-plan-regulatory-identifier-number-0648-bi04-july-2019.pdf/

PFMC (Pacific Fishery Management Council). 2019b. Salmon Rebuilding Plan for Queets River Natural Coho. Pacific Fishery Management Council, 7700 NE Ambassador Place, Suite 101, Portland, Oregon 97220-1384. Available from: https://www.pcouncil.org/documents/2019/10/queets-river-natural-coho-salmon-rebuilding-plan-regulatory-identifier-number-0648-bj05-october-2019.pdf/

PFMC (Pacific Fishery Management Council). 2019c. Salmon Rebuilding Plan for Sacramento River Fall Chinook. Pacific Fishery Management Council, 7700 NE Ambassador Place, Suite 101, Portland, Oregon 97220-1384. Available from: https://www.pcouncil.org/documents/2019/07/sacramento-river-fall-chinook-salmon-rebuilding-plan-regulatory-identifier-number-0648-bi04-july-2019.pdf/

PFMC (Pacific Fishery Management Council). 2019d. Salmon Rebuilding Plan for Snohomish River Natural Coho. Pacific Fishery Management Council, 7700 NE Ambassador Place, Suite 101, Portland, Oregon 97220-1384. Available from: https://www.pcouncil.org/documents/2019/10/snohomish-river-natural-coho-salmon-rebuilding-plan-regulatory-identifier-number-0648-bj05-october-2019.pdf/

PFMC (Pacific Fishery Management Council). 2019e. Salmon Rebuilding Plan for Strait of Juan de Fuca Natural Coho. Pacific Fishery Management Council, 7700 NE Ambassador Place, Suite 101, Portland, Oregon 97220-1384. Available from: https://www.pcouncil.org/documents/2019/10/strait-of-juan-de-fuca-natural-coho-salmon-rebuilding-plan-regulatory-identifier-number-0648-bj05-october-2019.pdf/

PFMC (Pacific Fishery Management Council). 2019f. Coastal Pelagic Species Fishery Management Plan as Amended through Amendment 17. PFMC, Portland, OR. 49 p. Available from: https://www.pcouncil.org/documents/2019/06/cps-fmp-as-amended-through-amendment-17.pdf/

PFMC (Pacific Fishery Management Council). 2020. Scientific and Statistical Committee Report on Pacific Sardine Rebuilding Plan – Final Action. PFMC, Portland, OR. 12 p. Available from: https://www.pcouncil.org/documents/2020/09/g-1-a-supplemental-ssc-report-1-2.pdf

Punt, A.E., and R.D. Methot. 2005. The impact of recruitment projection methods on forecasts of rebuilding rates for overfished marine resources. In: G. Kruse, V.F. Gallucci, D.E. Hay, R.I. Perry, R.M. Peterman, T.C. Shirley, P.D. Spencer, B. Wilson, and D. Woodby (eds.), Fisheries assessment and management in data-limited situations. Alaska Sea Grant, University of Alaska Fairbanks, pp. 571-594

Punt, A.E. and S. Ralston. 2007. A management strategy evaluation of rebuilding revision rules for overfished rockfish stocks. In Proceedings of the 2005 Lowell Wakefield Symposium-biology, Assessment, and Management of North Pacific Rockfishes (pp. 329-351).

R Core Team. 2019. R: a language and environment for statistical computing, Vienna, Austria. R Foundation for Statistical Computing. Available from: *https://www.r-project.org/*

Wetzel, C.R., and A.E. Punt. 2016. The impact of alternative rebuilding strategies to rebuild overfished stocks. ICES Journal of Marine Science 73, 2190–2207. https://doi.org/10.1093/icesjms/fsw073

Winship, A. J., M. R. O'Farrell, and M. S. Mohr. 2013. Management strategy evaluation applied to the conservation of an endangered population subject to incidental take. Biological Conservation 158, 155–166. http://dx.doi.org/10.1016/j.biocon.2012.08.031

Winship, A. J., M. R. O'Farrell, W. H. Satterthwaite, B. K. Wells, and M. S. Mohr. 2015. Expected future performance of salmon abundance forecast models with varying complexity. Canadian Journal of Fisheries and Aquatic Sciences 72, 557-569. http://dx.doi.org/10.1139/cjfas-2014-0247

Figure Captions

Figure 1. Number of salmon stocks that meet the criteria for overfished status in the West Coast Salmon Fishery Management plan (FMP), 1973-2018. Results are for 25 Chinook and coho salmon stocks that have a specified Minimum Stock Size Thresholds (MSST). Prior to 1992, data were not available for all 25 stocks and thus bars represent the minimum number of stocks meeting criteria for overfished status.

Figure 2. Abundance-based exploitation rate control rule used for data simulation and application within the rebuilding time model. A description of numerical break points for this control rule can be found in PFMC (2016).

Figure 3. Exploitation rate control rule rebuilding Alternatives for Sacramento River fall Chinook. Alternative I (solid line) represents the status quo control rule. Alternative II (dashed line) reflects reduced exploitation rates relative to Alternative I at all levels of forecast abundance. Alternative III (not depicted) is an exploitation rate of zero.

Figure 4. Estimates of the lag-1 autocorrelation coefficient ($\hat{\rho}$; A, B), log mean abundance [$\log(\bar{X})$; C, D], and the standard deviation of log-scale abundance [$\hat{\sigma}_{\log(X)}$, E, F] plotted against parameter values assumed for the simulated data series (horizontal lines). Results shown for abundance data length of 30 years (A, C, E) and 15 years (B, D, F) under three values of the lag-1 autocorrelation coefficient (ρ).

Figure 5. Raw error between model-projected and simulated rebuilding times under two scenarios of data series length and three scenarios of the level of lag-1 autocorrelation (ρ). Medians are represented by within-box horizontal lines and means are represented by diamonds. Raw error values outside of plot whiskers (1.5 times the interquartile range) were omitted for clarity.

Figure 6. Raw error between model-projected and simulated rebuilding times under two scenarios of data series length and three scenarios of the level of lag-1 autocorrelation. Rebuilding times were simulated with values of $\mathrm{CV}_{\hat{N}}$ (A), CV_{F} (B), and $\mathrm{CV}_{\hat{E}}$ (C) that exceeded values assumed in the rebuilding time model. Panel D displays raw errors when parameters $\mathrm{CV}_{\hat{N}}$, CV_{F}, and $\mathrm{CV}_{\hat{E}}$ all exceeded assumed values simultaneously. Medians are represented by within-box horizontal lines and means are represented by diamonds. Raw error values outside of plot whiskers (1.5 times the interquartile range) were omitted for clarity.

Figure 7. The effect of lag-1 autocorrelation on rebuilding time. Simulated rebuilding times are plotted as function of the underlying level of lag-1 autocorrelation assumed for simulations (A). Rebuilding times outside of plot whiskers (1.5 times the interquartile range) were omitted for clarity. Model-projected rebuilding time are plotted as a function of the lag-1 autocorrelation coefficient estimated from simulated data under the 30 year data series scenario (B). Horizontal lines in panel B indicate median rebuilding times over the range of estimated autocorrelation coefficients, in increments of 0.2.

Figure 8. Probability of achieving rebuilt status under each management strategy alternative and year for five overfished salmon stocks. The $\mathrm{T_{MIN}}$ strategy is based on an exploitation rate of zero (no ocean or freshwater fisheries). The horizontal gray lines indicate a probability of 0.5.

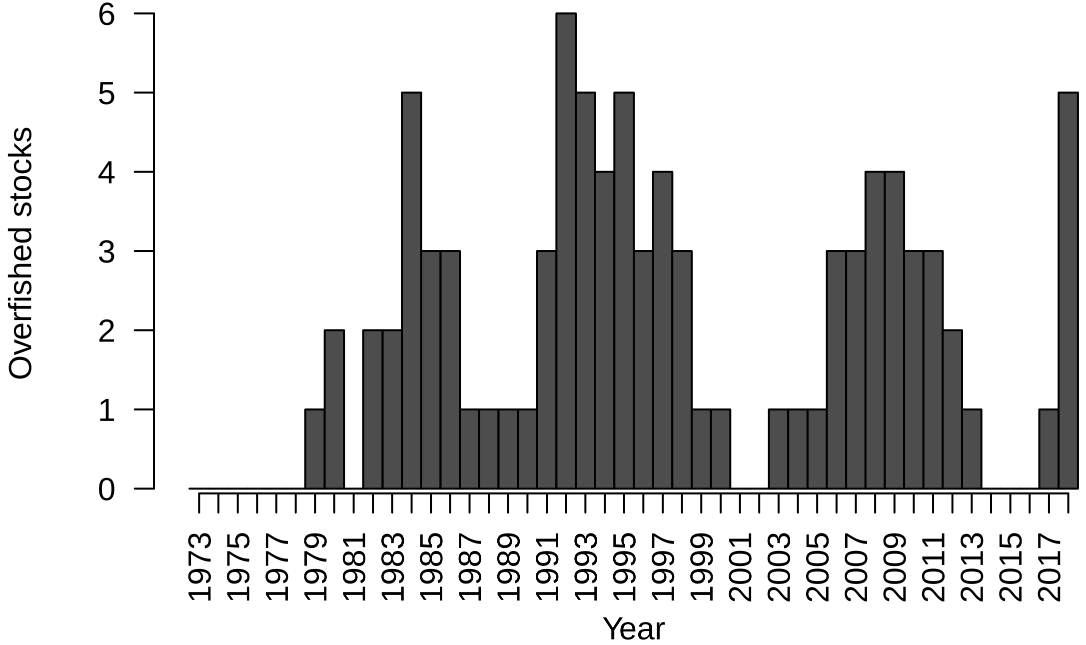

Overfished stocks
0
1
2
3
4
5
6
1973
1975
1977
1979
1981
1983
1985
1987
1989
1991
1993
1995
1997
1999
2001
2003
2005
2007
2009
2011
2013
2015
2017
Year

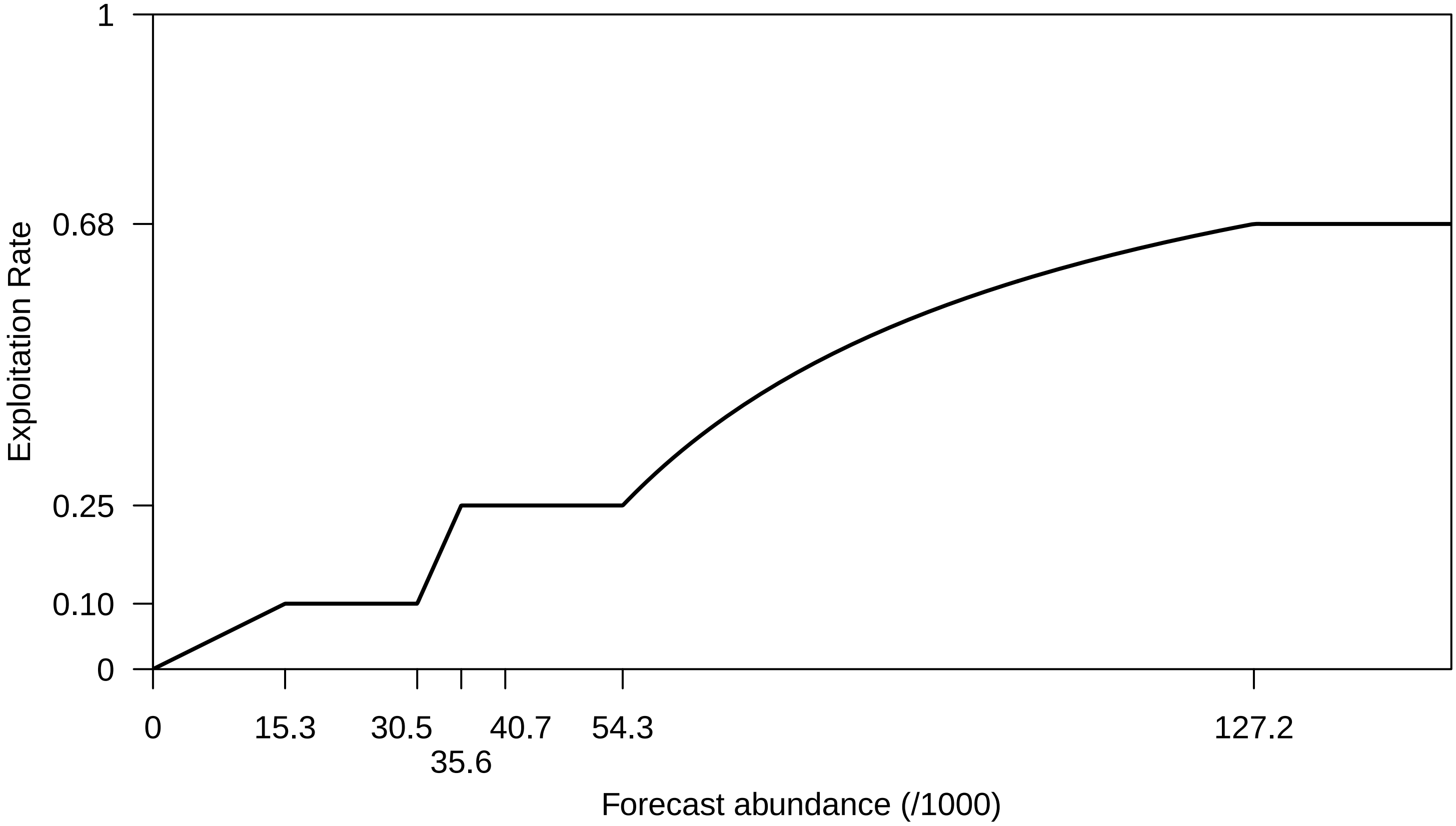
1
0.68
0.25
0.10
0
Exploitation Rate
0
15.3
30.5
35.6
40.7
54.3
127.2
Forecast abundance (/1000)

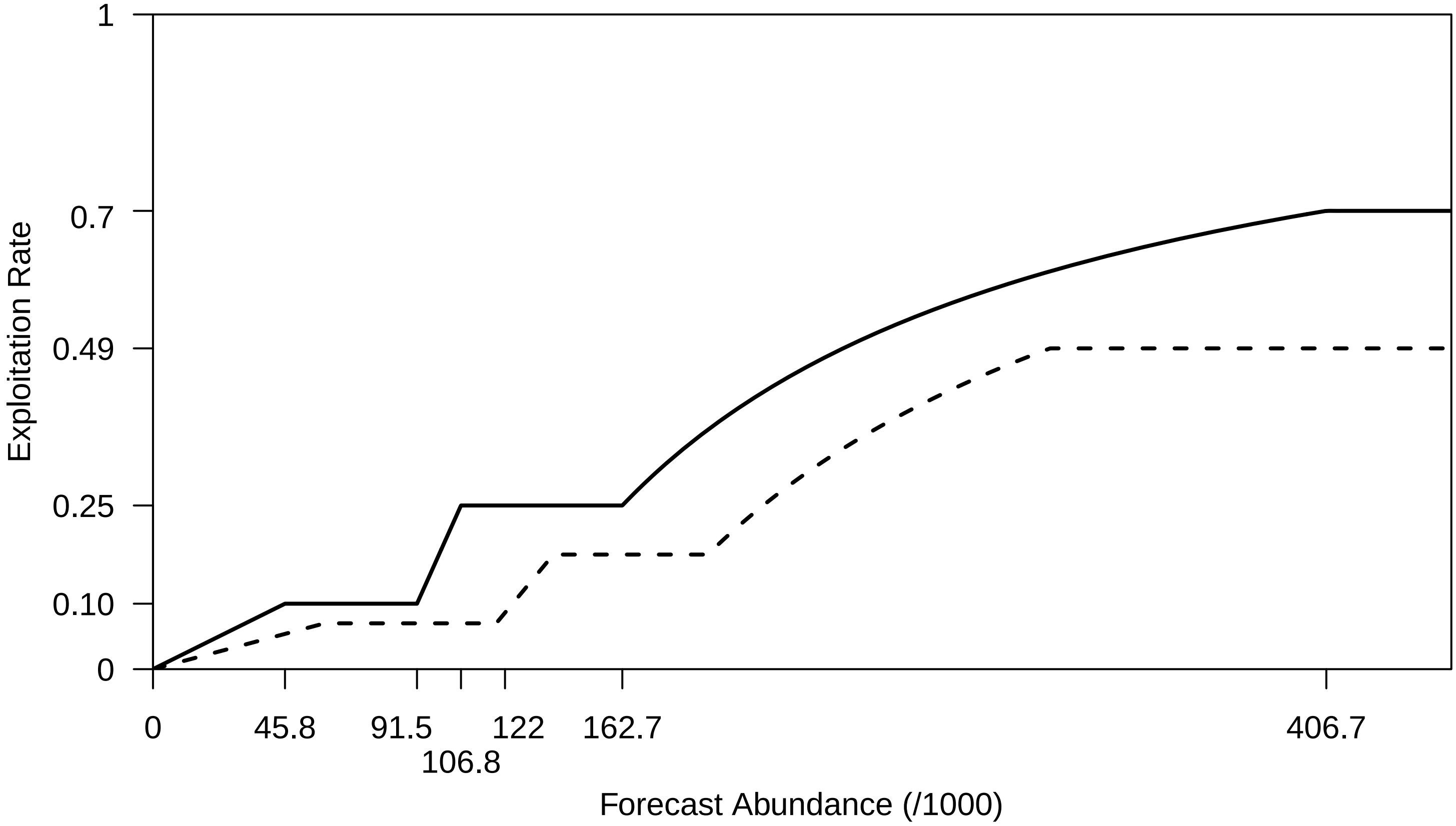
1
0.7
0.49
0.25
0.10
0
Exploitation Rate
0
45.8
91.5
106.8
122
162.7
406.7
Forecast Abundance (/1000)

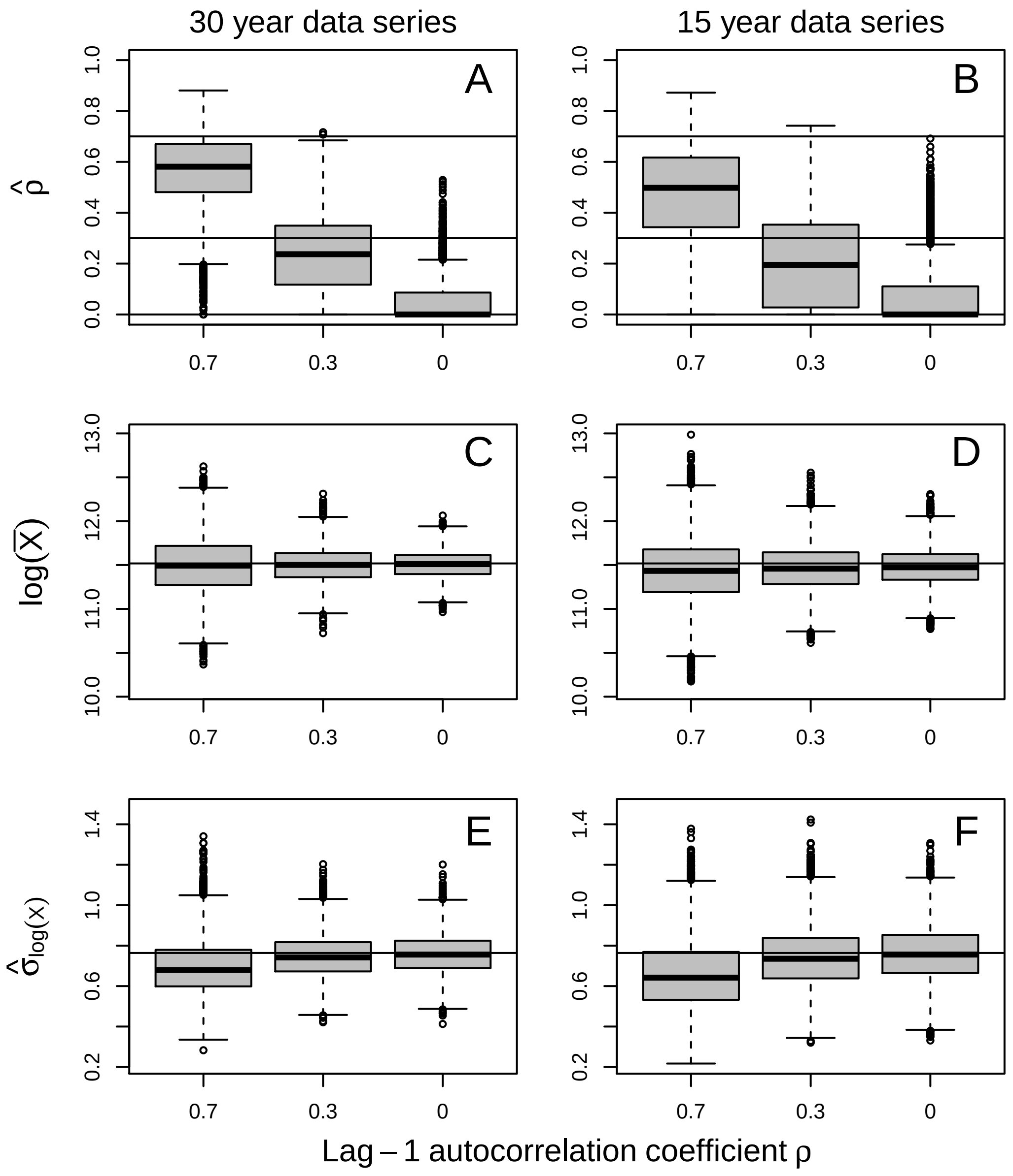

30 year data series
15 year data series
A
B
C
D
E
F
$\hat{\rho}$
$\log(\bar{X})$
$\hat{\sigma}_{\log(X)}$
1.0
0.8
0.6
0.4
0.2
0.0
13.0
12.0
11.0
10.0
1.4
1.0
0.6
0.2
0.7
0.3
0
Lag – 1 autocorrelation coefficient ρ

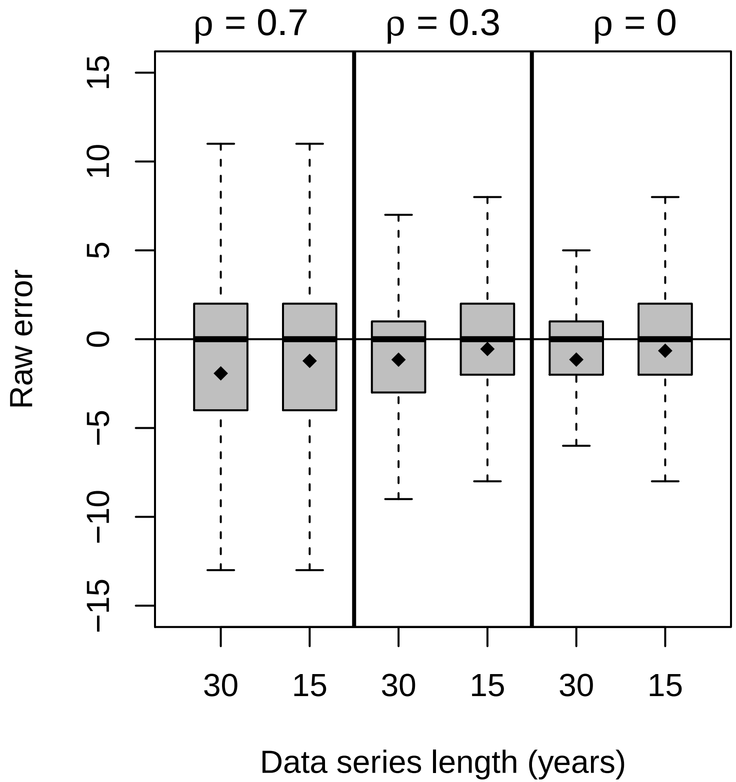
ρ = 0.7
ρ = 0.3
ρ = 0
15
10
5
0
−5
−10
−15
Raw error
30
15
30
15
30
15
Data series length (years)

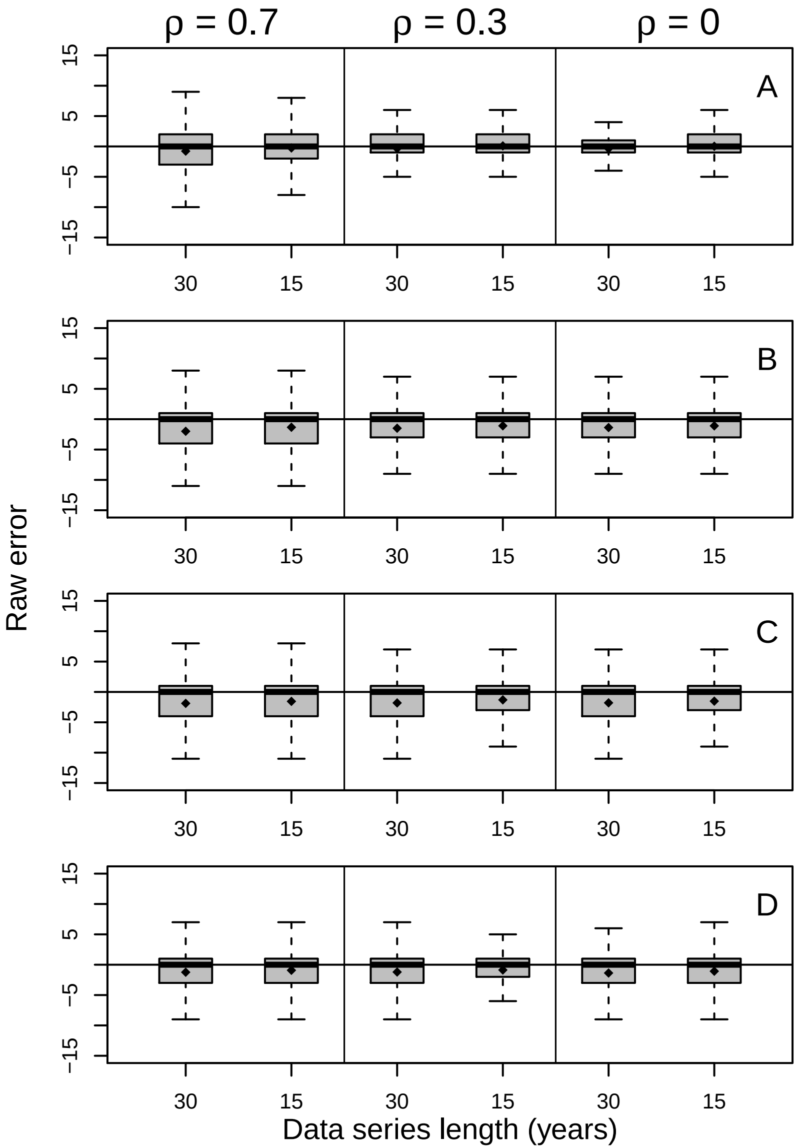
ρ = 0.7
ρ = 0.3
ρ = 0
A
B
C
D
Raw error
15
5
−5
−15
30
15
Data series length (years)

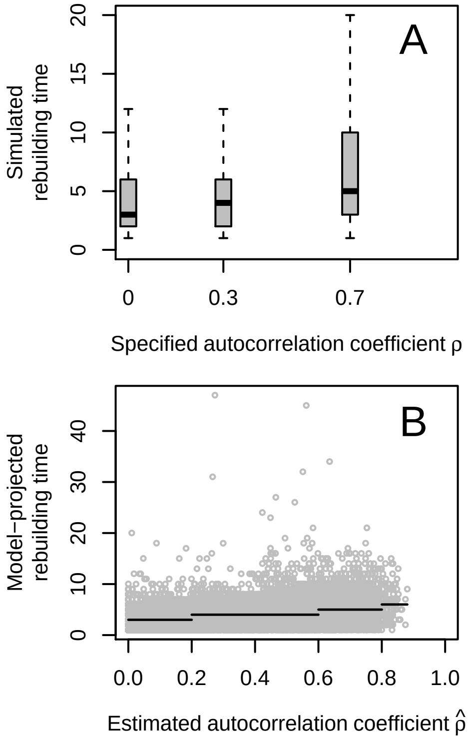
A
Simulated rebuilding time
0
5
10
15
20
0
0.3
0.7
Specified autocorrelation coefficient ρ
B
Model−projected rebuilding time
0
10
20
30
40
0.0
0.2
0.4
0.6
0.8
1.0
Estimated autocorrelation coefficient $\hat{\rho}$

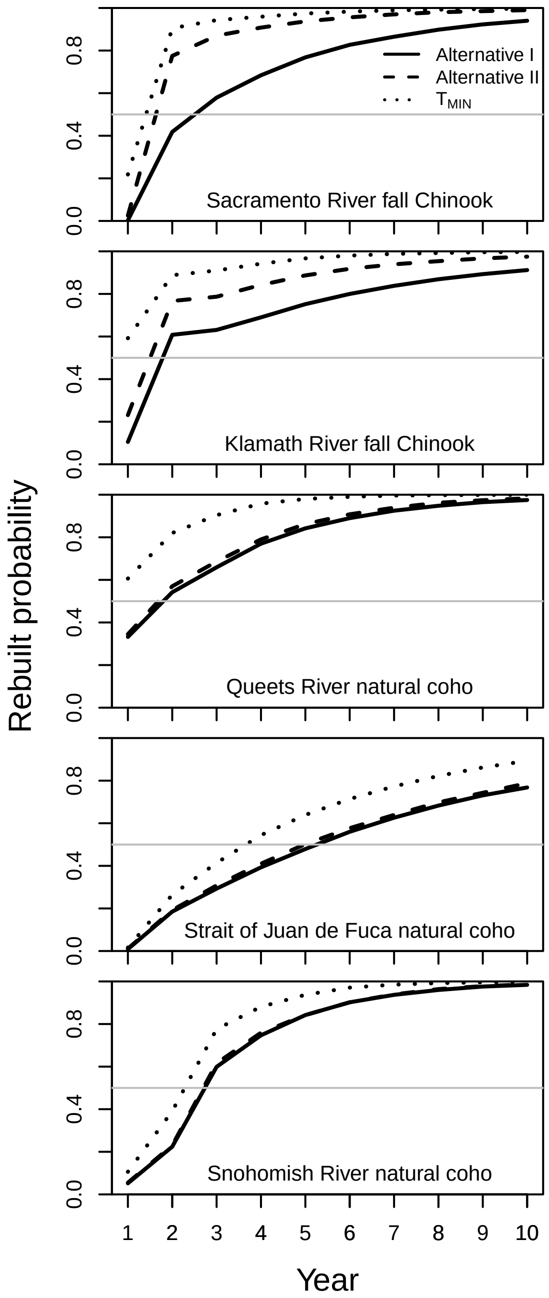
Rebuilt probability
Year
Alternative I
Alternative II
T_{MIN}
Sacramento River fall Chinook
Klamath River fall Chinook
Queets River natural coho
Strait of Juan de Fuca natural coho
Snohomish River natural coho
0.0
0.4
0.8
1
2
3
4
5
6
7
8
9
10